Rev Esp Cardiol. 2023;76(3):173–182

Original article

Quantification of right atrial fibrosis by cardiac magnetic resonance: verification of the method to standardize thresholds

Clara Gunturiz-Beltrán,[a,b,c] Roger Borràs,[a,b,d] Francisco Alarcón,[a,b] Paz Garre,[a,b] Rosa M. Figueras i Ventura,[e] Eva M. Benito,[a,b] Gala Caixal,[a,b] Till F. Althoff,[a,f,g] José María Tolosana,[a,b] Elena Arbelo,[a,b] Ivo Roca-Luque,[a,b] Susanna Prat-González,[a,b] Rosario Jesús Perea,[a,b] Josep Brugada,[a,b] Marta Sitges,[a,b,c] Eduard Guasch,[a,b,c,◇] and Lluís Mont[a,b,c,◇,*]

[a] *Institut Clínic Cardiovascular, Hospital Clínic, Universitat de Barcelona, Barcelona, Spain*
[b] *Institut dInvestigacions Biomèdiques August Pi i Sunyer (IDIBAPS), Barcelona, Spain*
[c] *Centro de Investigación Biomédica en Red de Enfermedades Cardiovasculares (CIBERCV), Spain*
[d] *Centro de Investigación Biomédica en Red de Salud Mental (CIBERSAM), Spain*
[e] *ADAS3D Medical, S.L., Barcelona, Spain*
[f] *Department of Cardiology and Angiology, Charité-University Medicine Berlin, Charité Campus Mitte, Berlin, Germany*
[g] *German Centre for Cardiovascular Research (DZHK), Partner Site Berlin, Berlin, Germany*

Article history:
Received 5 March 2022
Accepted 23 June 2022
Available online 7 July 2022

Keywords:
atrial fibrillation
right atrium
fibrosis
magnetic resonance

A B S T R A C T

Introduction and objectives: Late gadolinium-enhanced cardiac magnetic resonance (LGE-CMR) allows noninvasive detection of left atrial fibrosis in patients with atrial fibrillation (AF). However, whether the same methodology can be used in the right atrium (RA) remains unknown. Our aim was to define a standardized threshold to characterize RA fibrosis in LGE-CMR.
Methods: A 3 Tesla LGE-CMR was performed in 53 individuals; the RA was segmented, and the image intensity ratio (IIR) calculated for the RA wall using 1 557 767 IIR pixels (40 994 ± 10 693 per patient). The upper limit of normality of the IIR (mean IIR + 2 standard deviations) was estimated in healthy volunteers (n = 9), and patients who had undergone previous typical atrial flutter ablation (n = 9) were used to establish the dense scar threshold. Paroxysmal and persistent AF patients (n = 10 each) were used for validation. IIR values were correlated with a high-density bipolar voltage map in 15 patients undergoing AF ablation.
Results: The upper normality limit (total fibrosis threshold) in healthy volunteers was set at an IIR = 1.21. In the postablation group, 60% of the maximum IIR pixel (dense fibrosis threshold) was calculated as IIR = 1.29. Endocardial bipolar voltage showed a weak but significant correlation with IIR. The overall accuracy between the electroanatomical map and LGE-CMR to characterize fibrosis was 56%.
Conclusions: An IIR > 1.21 was determined to be the threshold for the detection of right atrial fibrosis, while an IIR > 1.29 differentiates interstitial fibrosis from dense scar. Despite differences between the left and right atria, fibrosis could be assessed with LGE-CMR using similar thresholds in both chambers.

Cuantificación de la fibrosis auricular derecha mediante resonancia magnética cardiaca: verificación del método para la estandarización de umbrales

Palabras clave:
Fibrilación auricular
Aurícula derecha
Fibrosis
Resonancia magnética

R E S U M E N

Introducción y objetivos: La resonancia magnética cardiaca con realce tardío de gadolinio (RMC-RTG) permite la detección no invasiva de la fibrosis auricular izquierda en pacientes con fibrilación auricular (FA). Sin embargo, se desconoce si se puede utilizar la misma metodología en la aurícula derecha (AD). Nuestro objetivo fue definir un umbral estandarizado para caracterizar la fibrosis auricular derecha mediante RMC-RTG.
Métodos: Se realizaron RMC-RTG de 3 T en 53 personas; se segmentó la AD y se calculó la razón de intensidad de imagen (RII) para la pared de la AD utilizando 1.557.767 píxeles de RII (40.994 ± 10.693 por paciente). El límite superior de la normalidad de la RII (RII promedio + 2 desviaciones estándar) se estimó en voluntarios sanos (n = 9); para establecer el umbral de cicatriz densa, se utilizó a los pacientes que se habían sometido previamente a una ablación del *flutter* auricular típico (n = 9). Se incluyó a pacientes con FA paroxística y persistente (n = 10 cada grupo) para la validación. Los valores de RII se correlacionaron con un mapa de voltaje bipolar de alta densidad en 15 pacientes sometidos a ablación de FA.

* Corresponding author.
E-mail address: lmont@clinic.cat (L. Mont).
@LluisMont2

◇ These two authors share senior authorship.

https://doi.org/10.1016/j.rec.2022.06.010
1885-5857/

Resultados: El límite superior de la normalidad (umbral de fibrosis total) en voluntarios sanos se fijó en RII = 1,21. En el grupo postablación, el 60% del píxel de la RII máximo (umbral de fibrosis densa) se calculó como RII = 1,29. El voltaje bipolar endocárdico mostró una correlación con la RII débil pero significativa. La precisión general entre el mapa electroanatómico y la RMC-RTG para caracterizar la fibrosis fue del 56%.

Conclusiones: Se determinó una RII > 1,21 como umbral para la detección de fibrosis de la aurícula derecha, mientras que una RII > 1,29 diferencia la fibrosis intersticial de la cicatriz densa. A pesar de las diferencias entre las aurículas izquierda y derecha, se pudo evaluar la fibrosis con RMC-RTG con umbrales similares en ambas cámaras.

Abbreviations

AF: atrial fibrillation
EAM: electroanatomical map
IIR: image intensity ratio
LGE-CMR: late gadolinium-enhanced cardiac magnetic resonance
RA: right atrium

INTRODUCTION

Atrial fibrosis is a determinant in the pathogenesis of atrial fibrillation (AF). Technical advances in recent years have enabled noninvasive characterization of atrial fibrosis by means of late gadolinium-enhanced cardiac magnetic resonance (LGE-CMR),1 fostering numerous potential clinical applications. LGE-CMR may be useful to personalize AF ablation with both first[2] and re-do[3] procedures benefitting from previous characterization of atrial fibrosis.[4] Discontinuities (gaps) in anatomical lesions induced by ablation have been shown to predict AF recurrences.[5] Finally, LGE-CMR could aid in selecting patients needing chronic anticoagulation for primary prevention of stroke.[6] However, the lack of standardized algorithms for fibrosis assessment and their variable reproducibility have limited the uptake and widespread use of LGE-CMR in clinical practice[7].

There are anatomical, functional, and molecular differences between the left atrium (LA) and the right atrium (RA). The contribution of the RA to AF pathology remains disputed, but clinical insights underpin a central role of the RA in some patients. The RA may be particularly sensitive to damage inflicted by sleep apnea and other respiratory diseases,[8,9] and ectopic foci sustaining AF have occasionally been localized in the RA.[10] Unfortunately, our knowledge on the contribution of the RA to AF substrate is, at least in part, jeopardized by technical limitations. For example, efforts in recent years have been directed towards the noninvasive identification of atrial fibrosis in the LA, but no study has yet tested whether similar algorithms are applicable to the RA. Few small studies have employed CMR to measure fibrosis in the RA, including a case series.[11] In patients with AF and sinus node dysfunction, Akoum et al.[12] found that fibrosis burden was higher in the left than in the right atrium. However, these algorithms had never been validated for RA fibrosis assessment.

Our objective was to define and validate a standardized, systematic, reproducible, and robust method to identify myocardial fibrosis in the RA by mean of LGE-CMR.

METHODS

The study protocol conforms to the Declaration of Helsinki and was approved by the research ethics committee of our institution (HCB/2018/0382). All patients provided signed informed consent. The data that support the findings of this study are available from the corresponding author, upon reasonable request. A comprehensive description of the methods is provided in the supplementary data.

Study design and cohorts under study

A systematic, sequential workflow[13] was used in different cohorts (figure 1) to determine RA wall intensity, differentiating healthy from fibrotic tissue as well as interstitial fibrosis from dense scar. This descriptive technical study was meant to lay the foundations for the interpretation of fibrosis measured by LGE-CMR in RA (figure 2).

A total of 53 individuals who had undergone LGE-CMR were included in consecutive stages of this study. Initially, thresholds to identify fibrosis in the RA were determined in healthy volunteers (individuals aged 18-30 years who had been recruited to assess LA fibrosis threshold,[13] n = 9) and patients who had undergone typical atrial flutter and AF ablation in the same procedure (n = 9, LGE-CMR performed 3 months postablation). Later, patients with paroxysmal (n = 10) or persistent (n = 10) AF were used for validation (LGE-CMR obtained 2 weeks before the ablation procedure). Finally, correlation between the image intensity ratio (IIR) and the electroanatomical bipolar voltage map (EAM) was evaluated in an additional prospective cohort of patients undergoing a first AF ablation procedure (n = 15).

Both the RA and LA were segmented from 3 Tesla (T) LGE-CMR (Magnetom Prisma Siemens Healthcare, Germany) images with ADAS 3D software (figure 3), and 3D shells were built. Signal intensity from each pixel of the RA wall was normalized to the mean LA blood intensity to calculate the IIR. All IIR values were represented in histograms, and the total fibrosis threshold was set as the mean IIR value in the healthy volunteer group plus 2 standard deviations (SD), which ensured that ≈ 97.5% of all pixels in the healthy volunteers group fell below this threshold. The dense scar threshold was defined as the IIR value corresponding to 60% of the maximum normalized intensity pixel in the RA of patients who had undergone cavotricuspid isthmus ablation, as previously defined in the LA.[3] Overall, healthy tissue, interstitial fibrosis, and dense scar were derived from IIR values.

Finally, in 15 consecutive patients undergoing AF ablation, bipolar voltage in an intraprocedural high-density point-by-point EAM of the RA (Lasso or Pentarray catheters, CARTO 3, Biosense-Webster, USA) was correlated to IIR values. Only EAM points projected on the CMR shell less than 10 mm apart were used. Standard voltage thresholds of 0.1 mV and 0.5 mV were used to characterize atrial dense scar, interstitial fibrosis, and healthy tissue.

Statistical analysis

Continuous variables are shown as mean ± SD or median [interquartile range]) unless otherwise stated, and groups were

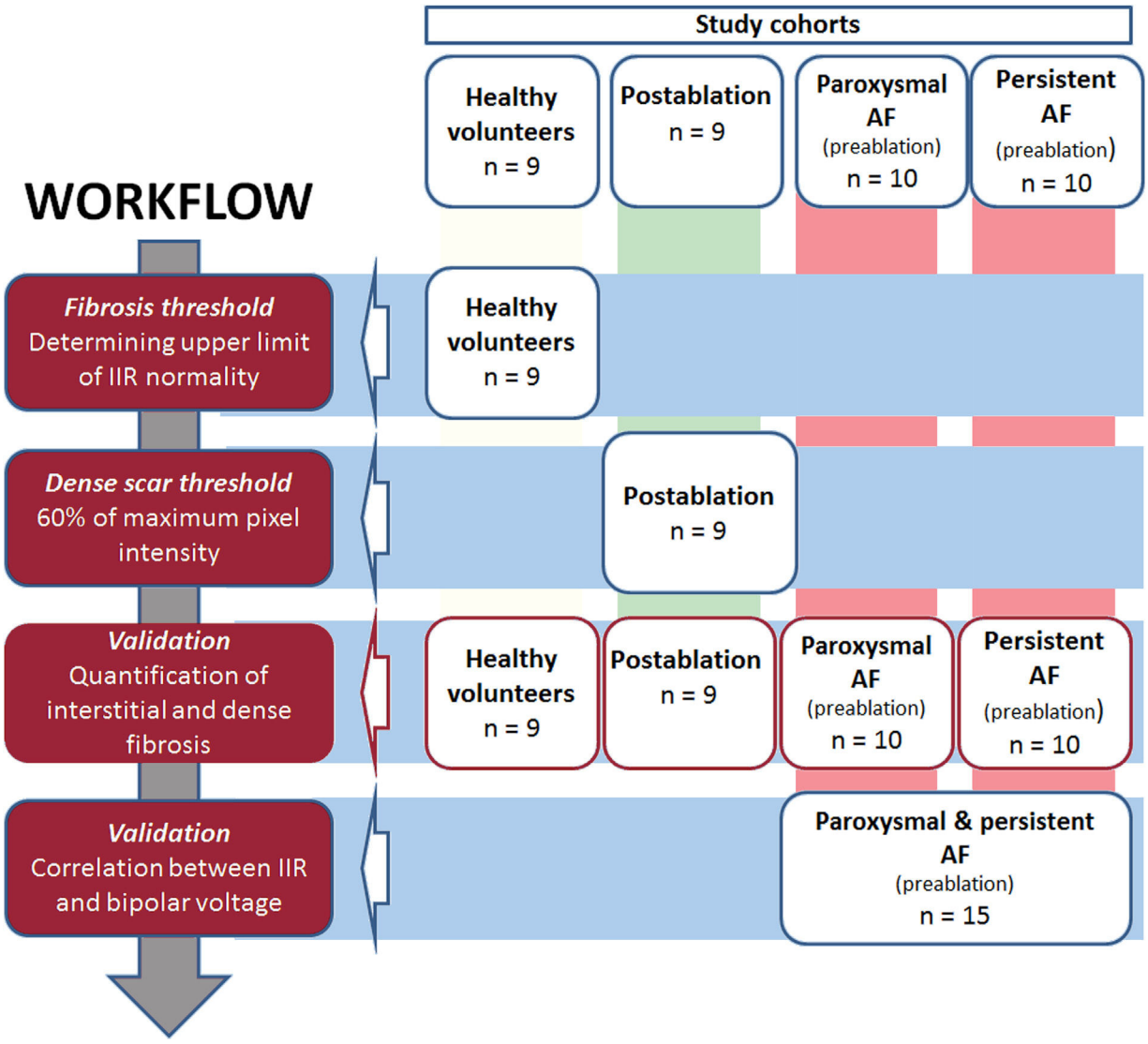

Figure 1. Workflow, cohorts used in the present study and summary of the workflow. AF, atrial fibrillation; IIR, image intensity ratio.

compared with 1-way ANOVA. The correlation between IIR and EAM was assessed using the Pearson correlation coefficient (r), and a generalized linear mixed model with random intercept accounted for repeated IIR measurements per patient. A 2-sided type I error of 5% was used for all tests. All analyses were performed using R v3.5.1 (R project for Statistical Computing).

RESULTS

Baseline characteristics of the population

The characteristics of the 4 study groups are shown in table 1. Most participants were male (71%). Young individuals with no risk factors were recruited for the healthy volunteer group. AF groups included middle-aged individuals with a similar burden of cardiovascular risk factors; structural heart disease was uncommon. Echocardiography was only available for AF patients and showed mild LA anteroposterior diameter enlargement (41 ± 6 mm). CMR showed a progressive enlargement of the RA from healthy volunteers to persistent AF.

Characterization of the pixel intensity in the RA

Overall, standardized LGE-CMR intensity values (ie, IIR) of 2 283 069 pixels were obtained from both atria of all participants: 1 557 767 pixels from the RA (40 994 ± 10 693 pixels per patient), and 725 302 pixels from the LA (19 087 ± 11 414 pixels per patient). When all participants were analyzed together, the average IIR was higher in the LA than in the RA (IIR 0.99; 95% confidence interval [95%CI], 0.97-1.02; vs 0.77; 95%CI, 0.74-0.79; respectively; $P < .0001$) (table 2).

Figure 4A shows the IIR histograms for the RA; LA histograms are provided for reference. We first characterized these histograms to determine how IIR values (ie, atrial fibrosis) were distributed on the RA. In all groups, the IIR histogram was asymmetric, with a long right tail distribution (mean skewness 0.64; a value of 0 denotes a symmetrical distribution) showing that some RA areas had very dense fibrotic patches. Patients with persistent AF had the smallest kurtosis (3.63; a kurtosis of 3 characterizes a normal distribution), revealing a larger dispersion of IIR values. Conversely, the larger kurtosis (4.66), reflecting a lower dispersion of IIR values around the mean, was observed in healthy volunteers.

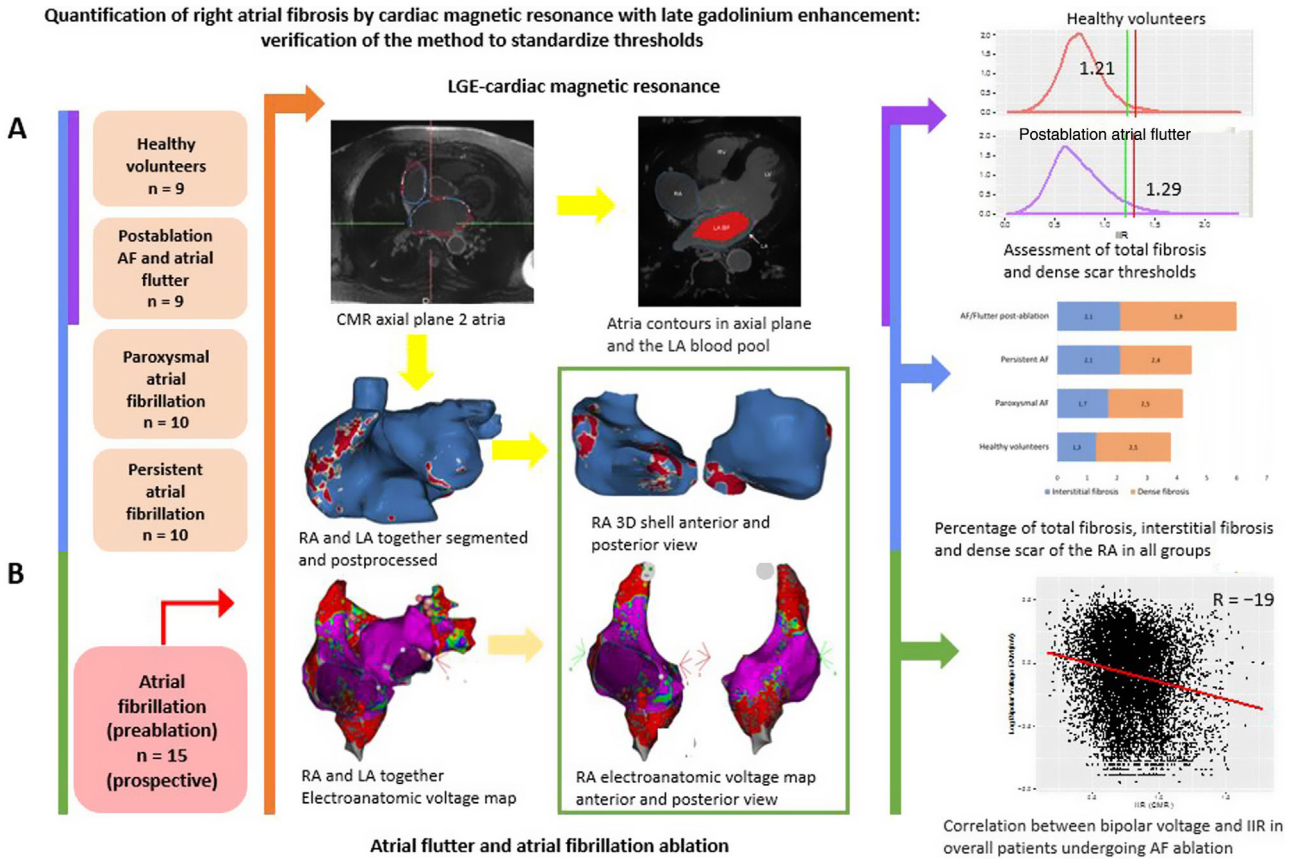

Figure 2. Central illustration. Quantification of right atrial fibrosis by cardiac magnetic resonance with late gadolinium enhancement. A: assessment of RA total fibrosis and dense scar thresholds in healthy volunteers and patients with typical atrial flutter and AF ablation in the same procedure, respectively. Application of the obtained thresholds to paroxysmal and persistent AF groups. B: correlation between LGE-CMR and electroanatomical map in a prospective group of patients undergoing AF ablation. AF, atrial fibrillation; CMR, cardiac magnetic resonance; IIR, image intensity ratio; LA, left atrium; LGE, late gadolinium enhancement; RA, right atrium.

Threshold determination

Normal IIR values of the RA myocardium were defined from healthy, young individuals. The upper limit of normality (mean IIR + 2SD) was calculated to be IIR = 1.21 (figure 4B). Therefore, all values with an IIR > 1.21 were considered to represent atrial fibrosis in the RA. Subsequently, the dense scar threshold was established in the group of patients who had undergone cavotricuspid isthmus ablation. As expected, in most cases, the maximum intensity pixel value in the RA was located in the cavotricuspid isthmus (figure 3B, bottom panel), while other high intensity pixels located superior and inferior cava vein, appendage, septum and peri-sinus coronary ostium (figure 5). Sixty percent of the maximum intensity pixel was calculated as IIR = 1.29, which was therefore used to discriminate interstitial fibrosis from dense scar (figure 4B).

Interindividual reproducibility was assessed with the interobserver Lin concordance correlation coefficient in a subset of 10 randomly selected right atria, segmented by 2 different independent observers. Correlation was 0.92 (0.68-0.98) for total fibrosis and 0.97 (0.89-0.99) for dense scar (table 3).

Validation of RA total fibrosis, interstitial fibrosis, and dense scar thresholds

The percentages of total, interstitial fibrosis and dense RA scar pixels were quantified in all groups to validate thresholds. The results are shown in table 4. Healthy volunteers had the lowest total RA fibrosis burden, followed by paroxysmal and persistent AF patients, and the largest amount of RA fibrosis was found in postablation patients. Subsequently, interstitial fibrosis and dense scar were quantified separately. Healthy volunteers and paroxysmal AF patients showed the least interstitial fibrosis, while persistent AF patients showed the most. Finally, postablation showed the largest dense scar, as expected. We found a strong association between interstitial fibrosis burden and the RA area (r = 0.84).

Correlation of EAM and CMR

A point-by-point correlation between the EAM and IIR of the RA was evaluated in 15 patients undergoing a first AF ablation procedure. Overall, 11 404 voltage values were registered, and 8 830 (407 (324-560)) points per patient remained after exclusion those located > 10 mm apart from the CMR shell. A weak but significant negative correlation was found between the log-transformed bipolar voltage and the IIR (r = −0.19; $P < .0001$ in the correlation analysis; beta = −1.39; 95%CI, −1.54 to −1.23; $P < .0001$ in generalized linear mixed modeling) (figure 6).

Subsequently, each of the EAM- and IIR-paired points were labelled as healthy tissue, interstitial fibrosis or dense scar, and agreement between the 2 was tested (table 5). In comparison with EAM, LGE-CMR tended to underestimate RA fibrosis (healthy tissue CMR 81.0%; 95%CI, 80.2-81.8 vs EAM 60.6%; 95%CI, 59.6-61.6 for

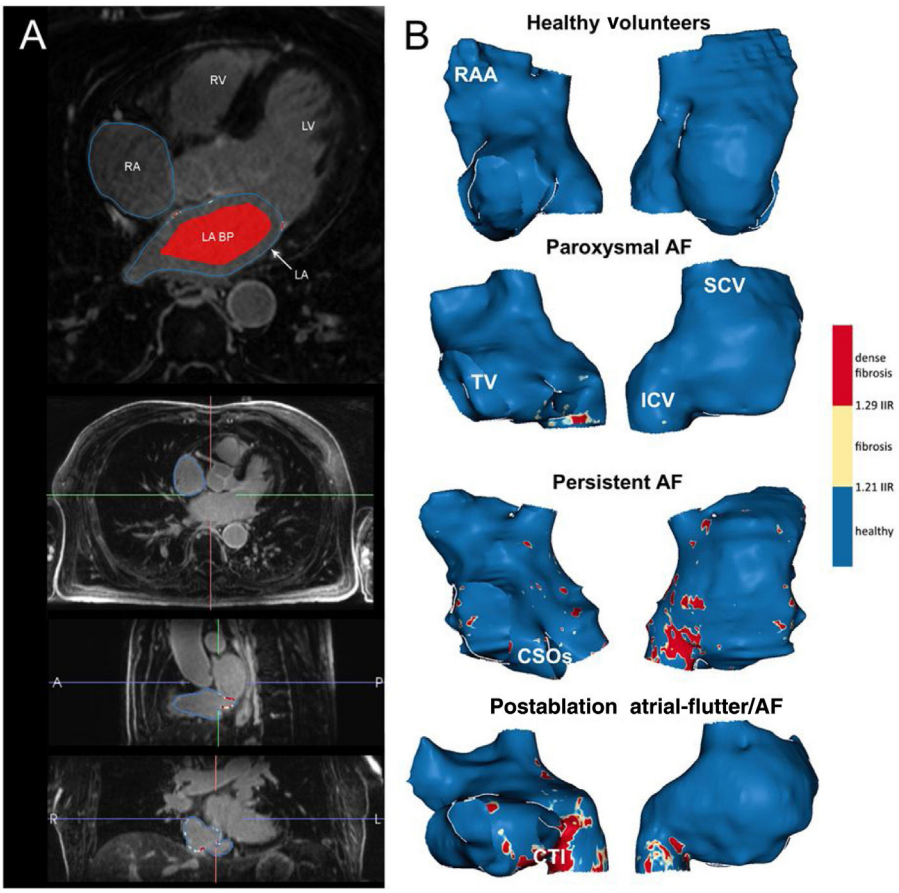

Figure 3. A: postprocessing of LGE-CMR images. In the upper panel, the RA and LA contours were drawn manually in an axial plane; the LA blood pool is shown in red. The 3 lower panels show axial, sagittal and coronal planes of a CMR during RA segmentation. B: anteroseptal (right) and posterolateral (left) views of representative examples of the RA in all the study groups. AF, atrial fibrillation; BP, blood pool; CSOs, coronary sinus ostium; CTI, cavo-tricuspid isthmus; ICV, inferior cava vein; LA, left atrium; LV, left ventricle; RA, right atrium; RAA, right atrium appendage; RV, right ventricle; SCV, superior cava vein; TV, tricuspid valve.

LGE-CMR and EAM, respectively). The overall agreement between the 2 techniques was 56%.

Then, bipolar voltage was averaged in each of the 3 LGE-CMR areas (eg, healthy tissue, interstitial fibrosis, dense scar). Bipolar voltage progressively increased from LGE-CMR-labelled areas as dense scar (mean EAM bipolar value 0.91 mV; 95%CI, 0.52-1.31) to interstitial fibrosis (1.11 mV; 95%CI, 0.72-1.50) to healthy tissue (1.77 mV; 95%CI, 1.40-2.15; $P < .0001$). Similarly, IIR progressively decreased from EAM-labelled areas as dense scar (mean IIR 0.87; 95%CI, 0.82-0.91) to interstitial fibrosis (IIR 0.81; 95%CI, 0.76-0-86) to healthy tissue (IIR 0.76; 95%CI, 0.72-0.81; $P < .0001$) (figure 7).

The left atria of the same 15 patients were used as a comparator for accuracy. In 15 479 EAM points (968 (700-1382) points per patient), we obtained a weak but significant negative correlation between the log-transformed bipolar voltage and the IIR ($r = -0.17$; $P < .0001$; beta $= -1.52$; 95%CI, -1.62 to -1.42; $P < .0001$), similar to results in the RA.

DISCUSSION

In this study, we describe a standardized method to assess RA fibrosis by means of LGE-CMR. Our results show that: *a)* an IIR > 1.21 characterizes myocardial fibrosis in the RA, while dense scar may be identified by an IIR > 1.29; and *b)* the IIR shows a weak but significant association with bipolar voltage in the RA.

LGE-CMR thresholds for atrial fibrosis are similar in the left and the right atria

Several methods have been proposed to characterize LA fibrosis.[1] The validated UTAH method[2] relies on the bimodal (healthy vs fibrosis) distribution of LA pixel intensity, but largely depends on the choice of an expert-led threshold.[14] The IIR was later designed to improve interindividual reproducibility.[15] Subsequently, characterization of healthy volunteers and patients who had undergone PV isolation enabled standardized categorization into healthy atrial myocardium, interstitial fibrosis, and dense scar.[13] We chose healthy volunteers at very low risk of AF (ie, aged less than 30 years) to minimize the degree of aging-induced interstitial fibrosis, thereby establishing a fibrosis threshold beyond which there is an increase in AF risk. Following an analogous approach, in the present study, we found that although IIR values characterizing fibrosis in the RA differed from those previously established for the LA, these differences were minor and, potentially, of little clinical relevance. Indeed, an IIR > 1.21 identified fibrosis in the RA, and an IIR > 1.29 differentiated interstitial fibrosis from dense scar, compared with an IIR > 1.20 and IIR > 1.32 for total fibrosis and dense scar in the LA, respectively. Structural, molecular, and functional differences between the left and right atria are evidenced by their distinct average IIR. However, despite these differences between the 2 atria,[16] fibrosis might be assessed with LGE-CMR using similar thresholds in both chambers.

Table 1
Characteristics of all the cohorts

	Healthy volunteers (n = 9)	Paroxysmal AF (n = 10)	Persistent AF (n = 10)	Postablation (n = 9)	Omnibus P (AF patients only)
Clinical data					
Male sex	4 (44)	8 (80)	8 (80)	7 (78)	.99
Age, y	26 ± 0	58 ± 10	57 ± 9	59 ± 8	.85
Hypertension	0 (0)	3 (30)	5 (50)	5 (56)	.49
Diabetes	0 (0)	0 (0)	1 (10)	1 (11)	.57
Sleep apnea	0 (0)	1 (10)	0 (0)	0 (0)	.41
Structural heart disease	0 (0)	0 (0)	1 (10)	4 (44)*	.03
Echocardiography					
LVEF, %	N/A	60 ± 7	59 ± 4	52 ± 10*	.03
LVEDD, mm	N/A	51 ± 4	49 ± 7	51 ± 5	.70
LA diameter, mm	N/A	38 ± 3	40 ± 7	45 ± 4*	.02
Magnetic resonance					
RA area, cm^2	94 ± 16	137 ± 30	149 ± 24	129 ± 25	.29
RA volume, mL	77 ± 20	121 ± 36	139 ± 38	104 ± 28	.10

AF, atrial fibrillation; LA, left atrium; LVEDD, left ventricular end diastolic diameter; LVEF, left ventricular ejection fraction.
Unless otherwise specified, values are expressed as count and percentage (qualitative variables) or as mean ± standard deviation (quantitative variables).
* $P < .05$ vs paroxysmal AF.

Table 2
Histogram descriptive values for the image intensity ratio of right and left atria

	Healthy volunteers	Paroxysmal AF	Persistent AF	Postablation
IIR				
RA	0.76 ± 0.23	0.77 ± 0.24	0.79 ± 0.24	0.73 ± 0.28
LA	0.94 ± 0.19	0.95 ± 0.21	1.01 ± 0.24	1.05 ± 0.26
Kurtosis				
RA	4.66	4.57	3.63	4.00
LA	11.70	3.76	4.52	5.46
Skewness				
RA	0.71	0.70	0.36	0.78
LA	1.31	-0.31	0.39	0.99

AF, atrial fibrillation; IIR, image intensity ratio; LA, left atrium; RA, right atrium; SD: standard deviation.
IIR values are expressed as mean ± standard deviation. Kurtosis and skewness are unitless parameters.

Interestingly, the correlation between EAM and CMR was statistically significant but of a weak intensity, similar to findings in the LA.[17] At least partially, such a low correlation might result from technical inaccuracies and other factors accounting for a decreased correlation, such as atrial size.[17] Of note, histological assessment is the only gold standard for atrial fibrosis assessment, but is not feasible in healthy individuals. The accuracy of atrial voltage to estimate atrial fibrosis is uncertain. It is likely that structural and functional data provided by CMR and EAM, respectively, yield complementary information on atrial remodeling. Finally, late gadolinium enhancement is found in fibrotic areas, but may also represent inflammation or portions of venous embryologic origin.

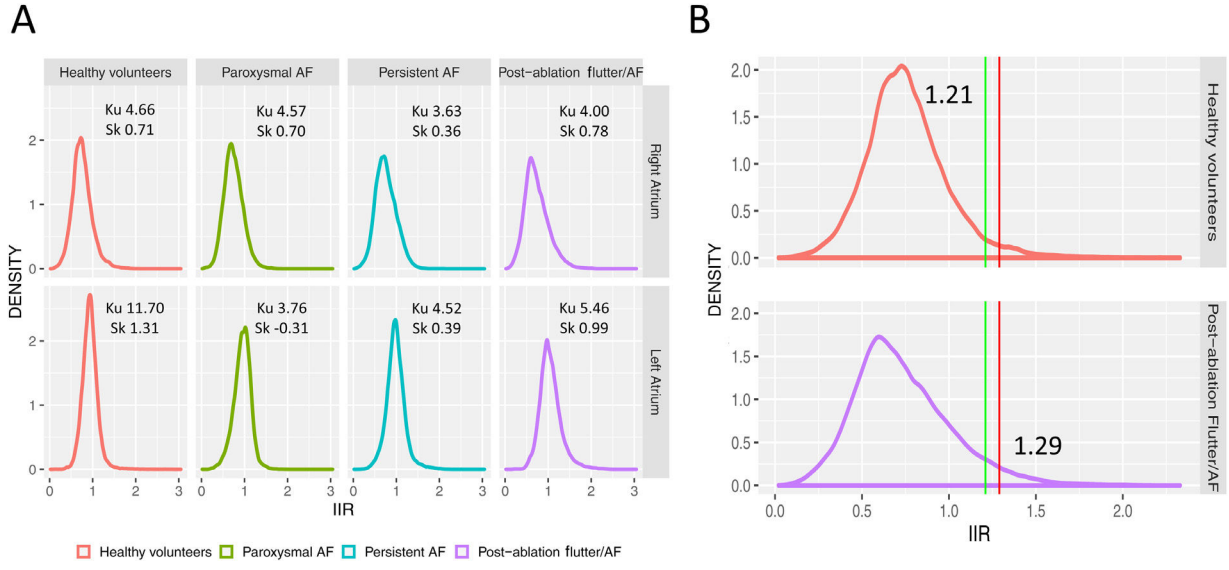

Figure 4. A: density distribution of IIR values for the RA and LA in all subgroups. B: identification of thresholds for healthy myocardial tissue (green line, measured in a healthy population) and dense scar (red line, measured in previously ablated patients) over RA histograms of all subgroups. AF, atrial fibrillation; IIR, image intensity ratio; Ku, kurtosis; Sk, skewness.

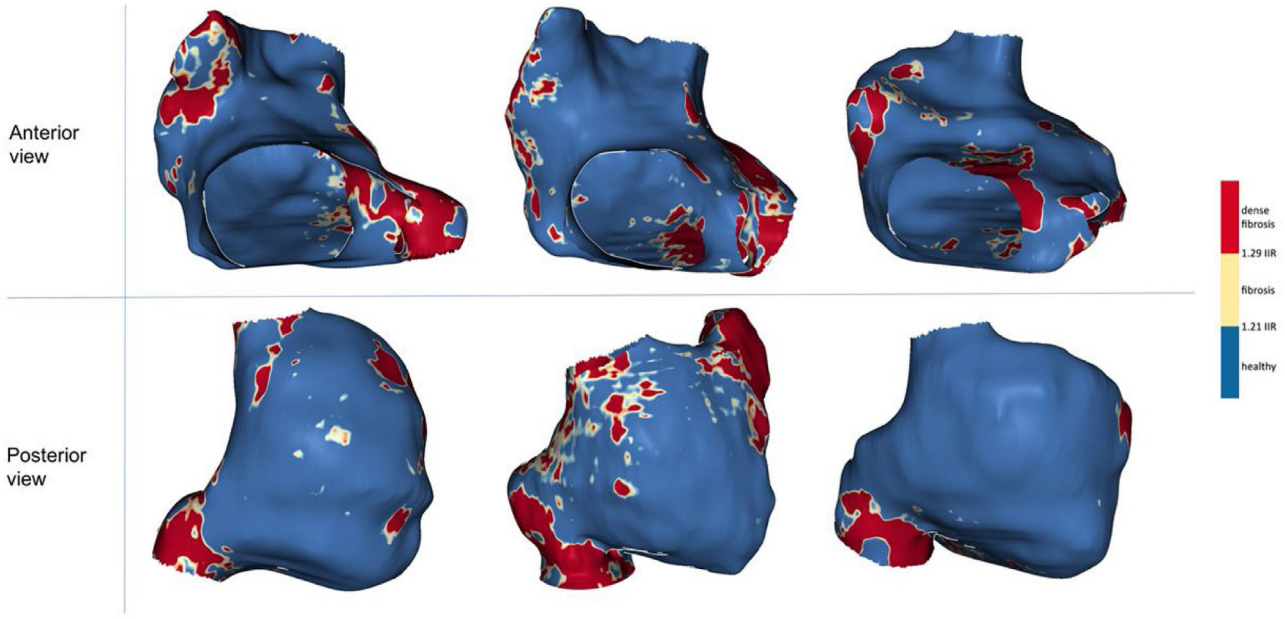

Figure 5. Examples of 3 CMR-LGE shells, depicting common high signal intensity areas in red. IIR, image intensity ratio.

Table 3
Fibrosis assessment reproducibility

	Total	Paroxysmal AF	Persistent AF
Lin concordance coefficient (95%CI)			
Total fibrosis	0.92 (0.68-0.98)	0.97 (0.63-1.00)	0.89 (0.20-0.99)
Dense scar	0.97 (0.89-0.99)	0.91 (0.64-0.98)	0.98 (0.83-1.00)

95%CI, 95% confidence interval; AF, atrial fibrillation.
The Lin concordance correlation coefficient was used to assess the agreement for total fibrosis and dense scar (for total sample and by type of AF) in 10 right atria segmented by 2 different independent observers.

Table 4
Total fibrosis, interstitial fibrosis and dense scar of the right atrium in all groups

	Total fibrosis	Interstitial fibrosis	Dense scar
Threshold	IIR > 1.21	1.21 <IIR ≤ 1.29	IIR > 1.29
Subgroup			
Healthy volunteers	3.78 (3.71-3.85)	1.28 (1.24-1.32)	2.50 (2.45-2.56)
Paroxysmal AF	4.19 (4.13-4.25)	1.68 (1.64-1.71)	2.52 (2.47-2.56)
Persistent AF	4.49 (4.44-4.55)	2.11 (2.07-2.15)	2.38 (2.34-2.43)
Postablation	5.97 (5.88-6.05)	2.07 (2.02-2.12)	3.90 (3.83-3.97)
P (omnibus)	< .001*	< .001*	< .001*

AF, atrial fibrillation; CI, confidence interval; IIR, image intensity ratio.
Values are expressed as percentage (95% confidence interval).
* *P* post hoc comparisons: all pairwise proportions comparisons were significant at the *P* < .001 level.

Right atrium fibrosis and remodeling in atrial fibrillation pathology

The driving role of the LA in sustaining AF in most patients is widely acknowledged. However, the RA also undergoes marked changes, and CMR,[12] computed tomography[18] and EAM[19] data suggest a similar remodeling intensity in both atria. In some cases, however, the RA might be particularly relevant to AF pathology and therapy. Some conditions superimpose an excessive pressure and volume overload in the RA.[20] Among AF patients, those with obstructive sleep apnea show decreased conduction velocity, lower electrogram voltage and a higher complexity in the RA than those without sleep apnea; notwithstanding, electrophysiological remodeling is also evident in sleep apnea patients.[9] In patients with atrial septal defects undergoing closure, RA dysfunction is a better predictor of incident AF than left atrial echocardiographic indices.[21] This may also hold true in settings such as congenital heart disease or reentrant arrhythmias after cardiac surgery, among others.

Overall, a "right origin AF", characterized by right atrial ectopia and a right-to-left dominant frequency gradient during AF, has been reported in some patients.[22,23] "Right AF" is associated with a

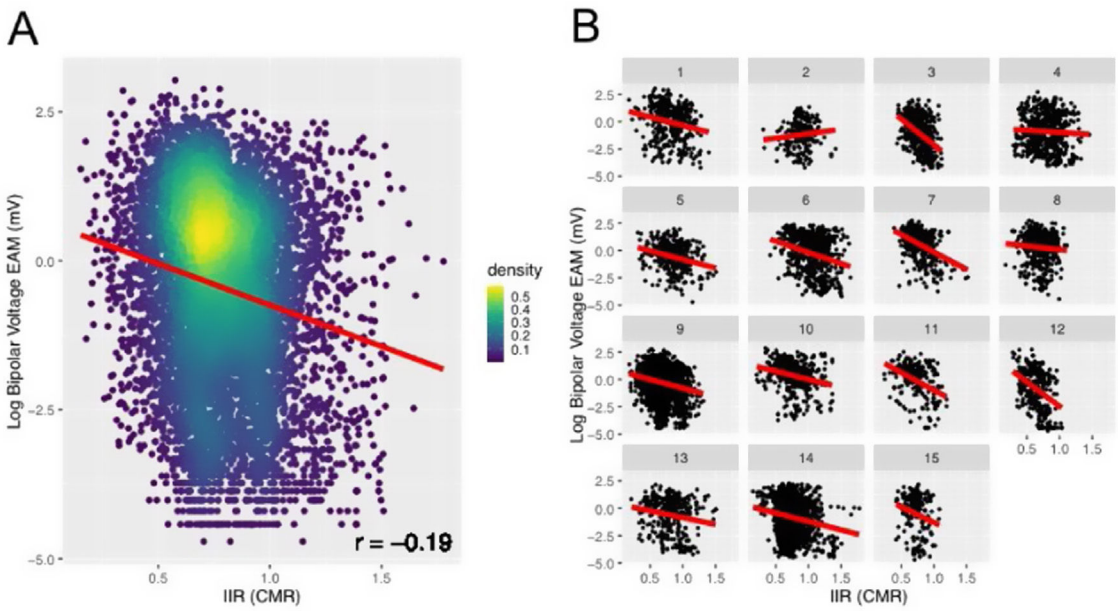

Figure 6. Correlation between bipolar voltage and IIR in the 15 patients undergoing AF ablation. A: overall correlation in the pooled cohort. Rather than a simple linear regression, the analysis was performed with a generalized linear mixed model with random intercept to account for repeated IIR measurements per patient. B: analysis at the patient level. CMR, cardiac magnetic resonance; EAM, electroanatomical map; IIR, image intensity ratio.

Table 5
Consistency between techniques in fibrosis categorization

	EAM (bipolar voltage)		
LGE-CMR (IIR)	Dense	Interstitial	Healthy
Dense	216	211	399
Interstitial	180	213	458
Healthy	1068	1592	4493

EAM, electroanatomical map; IIR, image intensity ratio; LGE-CMR, late gadolinium enhancement-cardiac magnetic resonance.
Values are expressed as count (number of pixels). Agreement between pixels classified as healthy tissue, interstitial fibrosis or dense scar in both the electroanatomical map (EAM) and the LGE-CMR.

smaller PV, LA, and left appendage, but a larger right appendage.[22] These data highlight the need for better characterization of the biatrial substrate in patients with AF. Our results will enable a more detailed, noninvasive characterization of RA fibrosis in patients with AF and, particularly, in those in which the RA could play a predominant pathophysiological role.

Clinical implications of right atrium fibrosis assessment

Myocardial fibrosis is a hallmark of AF pathology, and its characterization in daily clinical practice may have marked preventive, prognostic, and therapeutic implications. LGE-CMR has arisen as a potentially powerful tool to noninvasively assess atrial fibrosis, with most efforts focused on the LA. Unfortunately,

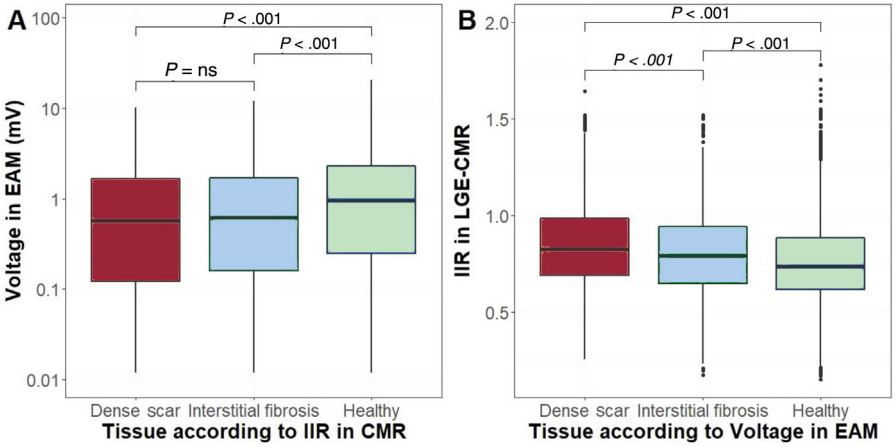

Figure 7. Comparative box plot charts (median and interquartile range values). A: bipolar voltage (EAM) in areas classified as healthy tissue, interstitial fibrosis, and dense scar by IIR (CMR). B: IIR values (CMR) in areas classified as healthy tissue, interstitial fibrosis, and dense scar by EAM. CMR, cardiac magnetic resonance; EAM, electroanatomical map; IIR, image intensity ratio.

data on an optimized method for RA fibrosis quantification has been lacking, so it remains underexplored.

The DECAAF trial proved that pre-existing LGE-CMR-detected LA fibrosis predicts postablation outcomes,[2] but it is unknown whether characterization of RA fibrosis yields additional information. Extra-PV foci sustaining AF have been found in approximately 20% of patients with AF, and in up to 35% of those with permanent AF.[10] Personalized ablation protocols targeting extra-PV fibrosis in the LA have been investigated in randomized clinical trials. Both the DECAAF II[24] and ALICIA[25] trials recently failed to show improved outcomes when fibrotic patches were targeted. However, ablation of non-PV foci arising from the superior and inferior vena cava, the crista terminalis, the foramen ovale and the coronary sinus ostium[10] has shown to terminate AF in some patients. Dedicated studies are needed to determine whether targeting LGE-CMR-detected RA fibrotic patches will serve to personalize ablation procedures.

Finally, the role of LA fibrosis estimation to flag those individuals at high risk of incident AF is still speculative, although supported by small studies.[26] If confirmed, patients with potentially "right AF" may benefit from RA fibrosis estimation. Testing for these potential applications warrant a dedicated, optimized, and refined methodology to quantify RA fibrosis; our findings are crucial for that purpose.

Limitations

Some limitations of our work should be acknowledged. Although blood pool normalization aims to compensate interindividual variability, other parameters may still account for significant variability in correlation analyses. Interelectrode distance, catheter disposition and mapping density might not be completely comparable among groups and could modify the results. Technical inaccuracies should not be disregarded. Registration errors in the EAM due to pressure on the atrial wall, or cardiac and respiratory movements may yield subtle changes in catheter position that could have a strong impact on correlation analyses. Correlation analyses were performed in a point-by-point basis in 3D shells; alternative flattening methods[27] or reducing the EAM-to-CMR tolerance distance (ie, 10 mm in our study) may yield more accurate correlations.[17]

The external reproducibility of our thresholds is critical to ensure wide clinical application of RA fibrosis assessment. We used a 3.0 T CMR setup that yields a high signal-to-noise ratio and improves image resolution. LA thresholds previously derived from 3.0 T Images [13] have been recently validated in 1.5 T setups;[28] whether RA thresholds may be applied in 1.5 T CMR setups needs to be proved. Similarly, images were obtained 20 minutes after gadolinium administration to reach enough image contrast;[29] shorter delays may result in different thresholds. Finally, our RA thresholds were obtained under specific parameters (see methods in the supplementary data) commonly used for LA fibrosis assessment, enabling the use of a single sequence for LA and RA fibrosis assessment; validity under different parameters cannot be ensured. We have recently shown good intra- and interobserver reproducibility even in the hands of inexperienced operators.[30]

CONCLUSIONS

The IIR threshold of the RA to determine healthy/fibrotic tissue was established at 1.21, close to the value used for the LA. Fibrosis quantification with CMR-LGE is feasible, and could be useful in both atria.

FUNDING

This work was supported in part by a grant from the European Union Horizon 2020 Research and Innovation Programme under grant agreement [No 633196] (CATCH ME project); *Instituto de Salud Carlos III* [PI16/00435, PI19/00573]; *Agència de Gestió d'Ajuts Universitaris i de Recerca* [AGAUR, 2017 SGR 1548]; *Fundació la Marató de TV3* [20152730]; CERCA Programme/*Generalitat de Catalunya*. The sponsor was not involved in the study design, data collection, analysis or interpretation of the results, the writing of the manuscript, or the decision to publish the work.

AUTHORS' CONTRIBUTIONS

C. Gunturiz-Beltrán: conceptualization, methodology, validation, formal analysis, investigation, resources, data curation, original draft writing, review of the draft and editing, visualization. R. Borràs: methodology, software, formal analysis. F. Alarcón, P. Garre, R. M. Figueras i Ventura: methodology, software. E.M Benito: conceptualization, methodology. G. Caixal, T.F, Althoff, J.M. Tolosana, E. Arbelo, I. Roca, J. Brugada: conceptualization, visualization. S. Prat-Gonzalez, R.J. Perea: software, visualization. M. Sitges: conceptualization, visualization, validation. E. Guasch: conceptualization, methodology, validation, formal analysis, investigation, resources, review of draft and editing, visualization, supervision. L. Mont: conceptualization, methodology, validation, resources, review of drafts and editing, supervision, project administration, funding acquisition. E. Guasch and L. Mont share senior authorship.

CONFLICTS OF INTEREST

L. Mont has received research grants, support for a fellowship program, and honoraria as a consultant and lecturer from Abbott, Boston Scientific, Medtronic, and Biosense, and is a shareholder for Galgo Medical S.L. M. Sitges has received research grants and honoraria as a consultant and speaker from Abbott, Medtronic, and Edwards Lifesciences. The remaining authors declare no conflicts of interest.

WHAT IS KNOWN ABOUT THE TOPIC?

- Atrial fibrosis is a determinant in the pathogenesis of AF as part of structural remodeling.
- LGE-CMR allows noninvasive characterization of atrial fibrosis and could be used to personalize AF ablation.
- Research has been focused on determining fibrosis in the LA, but no study has previously assessed right atrial fibrosis with magnetic resonance. This limits our ability to comprehensively characterize its contribution to AF pathology.

WHAT DOES THIS STUDY ADD?

- Thresholds identifying right atrial fibrosis in LGE-CMR: the IIR values above 1.21 identify total atrial fibrosis (interstitial fibrosis and dense scar, if present), and IIR values above 1.29 discern dense scar from interstitial fibrosis.
- IIR values to localize myocardial fibrosis are similar in the LA and RA.
- Endocardial bipolar voltage correlates with IIR in the RA.

APPENDIX. SUPPLEMENTARY DATA

Supplementary data associated with this article can be found in the online version, at https://doi.org/10.1016/j.rec.2022.06.010

REFERENCES

1. Oakes RS, Badger TJ, Kholmovski EG, et al. Detection and quantification of left atrial structural remodeling with delayed-enhancement magnetic resonance imaging in patients with atrial fibrillation. *Circulation.* 2009;119:1758–1767.
2. Marrouche NF, Wilber D, Hindricks G, et al. Association of atrial tissue fibrosis identified by delayed enhancement MRI and atrial fibrillation catheter ablation: the DECAAF study. *JAMA.* 2014;311:498–506.
3. Bisbal F, Guiu E, Cabanas-Grandío P, et al. CMR-guided approach to localize and ablate gaps in repeat AF ablation procedure. *JACC Cardiovasc Imaging.* 2014;7:653–663.
4. Segerson NM, Daccarett M, Badger TJ, et al. Magnetic resonance imaging-confirmed ablative debulking of the left atrial posterior wall and septum for treatment of persistent atrial fibrillation: rationale and initial experience. *J Cardiovasc Electrophysiol.* 2010;21:126–132.
5. Linhart M, Alarcon F, Borràs R, et al. Delayed Gadolinium Enhancement Magnetic Resonance Imaging Detected Anatomic Gap Length in Wide Circumferential Pulmonary Vein Ablation Lesions Is Associated With Recurrence of Atrial Fibrillation. *Circ Arrhythm Electrophysiol.* 2018;11:e006659.
6. Daccarett M, Badger TJ, Akoum N, et al. Association of left atrial fibrosis detected by delayed-enhancement magnetic resonance imaging and the risk of stroke in patients with atrial fibrillation. *J Am Coll Cardiol.* 2011;57:831–838.
7. Longobardo L, Todaro MC, Zito C, et al. Role of imaging in assessment of atrial fibrosis in patients with atrial fibrillation: State-of-the-art review. *Eur Heart J Cardiovasc Imaging.* 2014;15:1–5.
8. Caglar IM, Dasli T, Caglar FNT, Teber MK, Ugurlucan M, Ozmen G. Evaluation of atrial conduction features with tissue doppler imaging in patients with chronic obstructive pulmonary disease. *Clin Res Cardiol.* 2012;101:599–606.
9. Dimitri H, Ng M, Brooks AG, et al. Atrial remodeling in obstructive sleep apnea: implications for atrial fibrillation. *Heart Rhythm.* 2012;9:321–327.
10. Calkins H, Kuck KH, Cappato R, et al. 2012 HRS/EHRA/ECAS Expert Consensus Statement on Catheter and Surgical Ablation of Atrial Fibrillation: Recommendations for Patient Selection, Procedural Techniques, Patient Management and Follow-up, Definitions Endpoints, and Research Trial Design. *Heart Rhythm.* 2012;9:632–696.
11. Sato T, Tsujino I, Ohira H, et al. Right atrial late gadolinium enhancement on cardiac magnetic resonance imaging in pulmonary hypertension. *Circ J.* 2012;76:238–239.
12. Akoum N, McGann C, Vergara G, et al. Atrial fibrosis quantified using late gadolinium enhancement MRI is associated with sinus node dysfunction requiring pacemaker implant. *J Cardiovasc Electrophysiol.* 2012;23:44–50.
13. Benito EM, Carlosena-Remirez A, Guasch E, et al. Left atrial fibrosis quantification by late gadolinium-enhanced magnetic resonance: a new method to standardize the thresholds for reproducibility. *Europace.* 2017;19:1272–1279.
14. McGann CJ, Kholmovski EG, Oakes RS, et al. New Magnetic Resonance Imaging-Based Method for Defining the Extent of Left Atrial Wall Injury After the Ablation of Atrial Fibrillation. *J Am Coll Cardiol.* 2008;52:1263–1271.
15. Khurram IM, Beinart R, Zipunnikov V, et al. Magnetic resonance image intensity ratio, a normalized measure to enable interpatient comparability of left atrial fibrosis. *Heart Rhythm.* 2014;11:85–92.
16. Smorodinova N, Lantová L, Bláha M, et al. Bioptic Study of Left and Right Atrial Interstitium in Cardiac Patients with and without Atrial Fibrillation: Interatrial but Not Rhythm-Based Differences. *PLoS One.* 2015;10:e0129124.
17. Caixal G, Alarcón F, Althoff TF, et al. Accuracy of left atrial fibrosis detection with cardiac magnetic resonance: correlation of late gadolinium enhancement with endocardial voltage and conduction velocity. *Europace.* 2021;23:380–388.
18. Akutsu Y, Kaneko K, Kodama Y, et al. Association between left and right atrial remodeling with atrial fibrillation recurrence after pulmonary vein catheter ablation in patients with paroxysmal atrial fibrillation a pilot study. *Circ Cardiovasc Imaging.* 2011;4:524–531.
19. Prabhu S, Voskoboinik A, McLellan AJA, et al. A comparison of the electrophysiologic and electroanatomic characteristics between the right and left atrium in persistent atrial fibrillation: Is the right atrium a window into the left? *J Cardiovasc Electrophysiol.* 2017;28:1109–1116.
20. Houck CA, Lanters EAH, Heida A, et al. Distribution of Conduction Disorders in Patients With Congenital Heart Disease and Right Atrial Volume Overload. *J Am Coll Cardiol EP.* 2020;6:537–548.
21. Vitarelli A, Mangieri E, Gaudio C, Tanzilli G, Miraldi F, Capotosto L. Right atrial function by speckle tracking echocardiography in atrial septal defect: Prediction of atrial fibrillation. *Clin Cardiol.* 2018;41:1341–1347.
22. Hasebe H, Yoshida K, Iida M, et al. Differences in the structural characteristics and distribution of epicardial adipose tissue between left and right atrial fibrillation. *Europace.* 2018;20:435–442.
23. Hasebe H, Yoshida K, Iida M, Hatano N, Muramatsu T, Aonuma K. Right-to-left frequency gradient during atrial fibrillation initiated by right atrial ectopies and its augmentation by adenosine triphosphate: Implications of right atrial fibrillation. *Heart Rhythm.* 2016;13:354–363.
24. Marrouche NF, Wazni OM, Greene T, et al. DECAAF II: efficacy of DE-MRI-guided fibrosis ablation vs. conventional catheter ablation of persistent atrial fibrillation In: ESC Congress 2021–The Digital Experience 2021. 2022. Available at: https://esc365.escardio.org/presentation/238817?_ga=2.81001623.1615516082.1655647275-444216582.1639827571. Accessed 19 June 2022
25. Bisbal F, Benito E, Teis A, et al. Magnetic Resonance Imaging-Guided Fibrosis Ablation for the Treatment of Atrial Fibrillation: The ALICIA Trial. *Circ Arrhythm Electrophysiol.* 2020;13:e008707.
26. Peritz DC, Catino AB, Csecs I, et al. High-intensity endurance training is associated with left atrial fibrosis. *Am Heart J.* 2020;226:206–213.
27. Nunez-Garcia M, Bernardino G, Alarcon F, Caixal G, Mont L, Camara CBO. Fast Quasi-Conformal Regional Flattening of the Left Atrium. *IEEE Trans Vis Comput Graph.* 2020;26:2591–2602.
28. Bertelsen L, Alarcón F, Andreasen L, et al. Verification of threshold for image intensity ratio analyses of late gadolinium enhancement magnetic resonance imaging of left atrial fibrosis in 1.5 T scans. *Int J Cardiovasc Imaging.* 2020;36:513–520.
29. Chubb H, Aziz S, Karim R, et al. Optimization of late gadolinium enhancement cardiovascular magnetic resonance imaging of post-ablation atrial scar: a crossover study. *J Cardiovasc Magn Reson.* 2018;20:30.
30. Mrgulescu AD, Nuñez-Garcia M, Alarcón F, et al. Reproducibility and accuracy of late gadolinium enhancement cardiac magnetic resonance measurements for the detection of left atrial fibrosis in patients undergoing atrial fibrillation ablation procedures. *Europace.* 2019;21:724–731.